A numerical method for computing minimal surfaces in arbitrary dimension

Thomas Cecil*

June 25, 2004

Abstract

In this paper we propose a numerical method for computing minimal surfaces with fixed boundaries. The level set method is used to evolve a codimension-1 surface with fixed codimension-2 boundary in $\mathbb{R}^n$ under mean curvature flow. For $n = 3$ the problem has been approached in [3] using the level set method, but with a more complicated boundary condition. The method we present can be generalized straightforward to arbitrary dimension, and the framework in which it is presented is dimension independent. Examples are shown for $n = 2, 3, 4$.

1 Introduction

Given a fixed codimension-2 boundary Γ in $\mathbb{R}^n$, we would like to find a codimension-1 surface S of minimal surface area that takes Γ as its boundary. If we let S be the set $\{x|\varphi(x) = 0\}$ for a function $\varphi : \mathbb{R}^n \to \mathbb{R}$, then the surface area to be minimized can be written as

$$A = \int_{\mathbb{R}^n} |\nabla\varphi|\delta(\varphi)dx. \tag{1}$$

Applying the method of gradient descent to (1) we arrive at the evolution PDE

$$\varphi_t = \delta(\varphi)\nabla \cdot \left(\frac{\nabla\varphi}{|\nabla\varphi|}\right). \tag{2}$$

Within the level set framework it is advantageous to avoid the δ function and so the related PDE:

$$\varphi_t = |\nabla\varphi|\nabla \cdot \left(\frac{\nabla\varphi}{|\nabla\varphi|}\right), \tag{3}$$

that also evolves φ towards a minimizer of (1), is studied here. Evolution under (3) is known as mean curvature flow. The basic idea behind our technique is

*Department of Mathematics, University of California, Los Angeles, CA 90095-1555, USA. email: tcecil@math.ucla.edu

to initialize a surface that passes through Γ and then evolve it to steady state using (3), while forcing it at all times to span Γ.

The study and computation of minimal surfaces has a long history. Classical theory can be found in [5], [13]. Some of the first numerical approximations can be found in [6]. There has been much study in the dimension $n = 3$, and there are many finite element approaches [11], [9]. In [16] minimal surfaces were approximated by the level sets of functions of least gradient. Mean curvature flow was used in [7] to compute stable minimal surfaces using finite elements on surfaces. A network of marker particles is used in the works [1], [4], [18], and non-parametric representations were used in [12], [10]. See [8] for a more detailed listing.

A method proposed in [3] uses a similar level set framework for $n = 3$, but requires complicated boundary conditions for φ near Γ. These boundary conditions require the user to find the intersection of various lines and planes with Γ. Thus, an analytic representation of gamma must be given or constructed to find these intersections. Also, the boundary may be unable to avoid an inconsistent construction. The generalization of that method to higher dimensions is also not available.

Our method is similar to the method in [3] away from Γ, using finite difference methods for Hamilton-Jacobi equations [14], [15]. However, near Γ we use a different technique. To form the spatial derivatives on the right side of (3) we use a radial basis function (RBF) reconstruction of φ with stencil points that lie exactly on Γ. Then this reconstruction is differentiated to find the needed spatial derivatives. Therefore no analytic construction of Γ is needed, and the user only needs to know data points on the minimal surface boundary Γ. Because the RBF reconstruction is dimension independent, the method easily generalizes to arbitrary dimension and we have obtained results in $\mathbb{R}^4$.

The outline of the paper is as follows: we begin with the description of the evolution procedure away from Γ. Secondly, we discuss the RBF reconstruction and the procedure for evolution near Γ. Finally, numerical examples in $\mathbb{R}^n,\ n = 2, 3, 4$ are shown.

2 Evolution procedure away from Γ

2.1 Grid construction

First, we describe the procedure for constructing the computational domain. Given a fixed, compact, codimension-2 boundary in $\mathbb{R}^n$ we find an n-dimensional cube, $\Omega \supset \Gamma$, such that $\|\Gamma - \partial\Omega\| > \epsilon$, where ϵ is the size of a few (3 or 4) grid cells. This buffering is to ensure that the stencils used in calculating the terms in (3) do not cross $\partial\Omega$. Given Ω we discretize it using a uniform grid with distance between nodes $= dx$, and call this discretized set $\bar{\Omega}$.

2.2 Evolution of mean curvature flow

We treat the evolution of (3) using the method of lines. The time derivatives are calculated using TVD Runge-Kutta schemes [15].

The spatial derivatives are calculated using central finite differences. The curvature term can be written as

$$k \equiv \left[\sum_{i=1}^{n} \varphi_{x_i x_i} \left(\sum_{\substack{j=1 \\ j \neq i}}^{n} \varphi_{x_j}^2 \right) - \sum_{i=1}^{n} \sum_{\substack{j=1 \\ j \neq i}}^{n} \varphi_{x_i x_j} \varphi_{x_i} \varphi_{x_j} \right] / |\nabla \varphi|^3. \tag{4}$$

Second order finite differencing applied to (4) at a point x_0 results in a stencil S_0 of size 3^n, which consists of all the points $\{y|\ \|y - x_0\|_\infty \leq dx\}$. Finite differencing is also applied to the term $|\nabla \varphi|$.

When we say a point x_0 is "away from Γ," we mean:

1. There are no points $y \in \Gamma$ that lie in the cube $\{y|\ \|y - x_0\|_\infty < dx\}$, so that the convex hull of the stencil used in advancing (3) does not cross Γ.

2. That all points of S_0 are part of $\bar{\Omega}$. We say this here because in the next section we will explain how certain points of $\bar{\Omega}$ are removed from the computational domain if they are too close to Γ.

We use Neumann BCs $\partial u / \partial n = 0$ on $\partial \Omega$.

2.3 Reinitialization

Another procedure that must be applied at every timestep is reinitialization of φ to a distance function. This is done by evolving the PDE

$$\varphi_t + s(\varphi)(|\nabla \varphi| - 1) = 0, \tag{5}$$

where s is a smoothed version of the signum function. As this is done every timestep we only compute a few iterations of (5). See [15] for details on this computation on uniform grids.

3 Evolution procedure near Γ

In this section we describe the evolution of (3), (5) on the set of all points that are not "away from Γ."

3.1 Grid adjustment

Because of the possibility that a point $x_0 \in \bar{\Omega}$ could be very close to Γ we remove the set of points $B \equiv \{x|\ \|x - \Gamma\|_2 < d\}$ from $\bar{\Omega}$, where $d < dx$. We use $d = 0.5 * dx$ in practice. This is done so that CFL condition is not over restrictive. Thus our final computational grid consists of $(\bar{\Omega} \setminus B) \cup \Gamma$.

3.2 Evolution of mean curvature flow

Firstly, we note that as Γ is part of the minimal surface we set $\varphi(x \in \Gamma, t) = 0 \; \forall t$.

To evolve (3) at a point x_0 we form a local RBF reconstruction of φ, which we call Φ, and then differentiate Φ to find the spatial derivatives needed in (4) (which include the partial derivatives needed in $|\nabla\varphi|$). This reconstruction is done using a 3^n point stencil, S_0, found using the method of rays described in [2], with the rays given by $r_k = x_0 + v_k\tau, \; \tau \geq 0$, where v_k are taken to be all points on the unit cubic lattice $\mathbb{Z}^n$ with $\|v_k\|_\infty = 1$.

We will briefly describe the method again here.

Assume we have defined $N = 3^n$ rays, $r_k = x_0 + v_k\tau, \; \tau > 0, \|v_k\|_2 = 1$, emanating from x_0. We then find the neighbor x_j of x_0 that maximizes $V \equiv f(x_0, x_j, v_k, \bar{\Omega}, N)$.

The choice of the stencil preference function f has some flexibility. The general properties it should have are that it should be a non-increasing function of $\alpha = \cos^{-1}(\frac{x_j - x_0}{\|x_j - x_0\|_2} \cdot v_k)$, and $\beta = \|x_j - x_0\|$ (this norm can be chosen by the user). Also, f will depend on the local density of points, ρ_0, near x_0.

For example, in 2 dimensions if we calculate ρ_0 and we have chosen N, then we can define $f = g$ where

$$g \equiv \begin{cases} \cos\alpha & \text{if } \|x_j - x_0\|_2 < \sqrt{\frac{N}{\pi\rho_0}}, \\ -\infty & \text{otherwise} \end{cases}$$

Here we have derived the radius of the support of f, $R = \sqrt{\frac{N}{\pi\rho_0}}$, by equating $\rho = \frac{N}{\pi R^2}$. Thus we are assuming that the points in the ball $\|x_j - x_0\|_2 < R$ have approximate density ρ_0. To calculate ρ_0 we can use the number points in the neighboring coarse grid cells of x_0 divided by the total size of those cells. Other examples choices of f are g^p for $p > 0$, or $f = -\beta$, or combinations of these functions such as g/β or $g - \beta$. In practice we use $f = g - \beta/C$, where C is a scaling constant depending on the mesh size.

Some examples of choices of f are shown in figures 1, 2, and 3. For these examples $v_k = (0, 1)$. The function is shown on the left and its contour plot shown on the right in each figure for $0 \leq \alpha \leq \pi/2$. The scale for the x, y axes has been multiplied by 50. Figure 4 shows an example in 2d of how a single stencil node would be chosen. The contour lines of f are shown, along with v_0, $x_0 = (1, 1)$, and candidate stencil nodes $x_j, j = 1 : 4$. In this example the node that maximizes f is x_1.

Once S_0 is found we form our reconstruction Φ following the RBF parameter optimization procedure outlined in [2]. Next, approximations to the partial derivatives in (4) are constructed by taking second order central finite differences of Φ on a uniform grid that has minimal distance between nodes $= h$. In practice we use $h = dx$ or $h = 0.5\,dx$. This adds a small amount of numerical diffusion to the derivatives that is not present if we were to differentiate Φ exactly.

After the spatial derivatives are calculated, TVD Runge-Kutta time advancement is used to advance the solution.

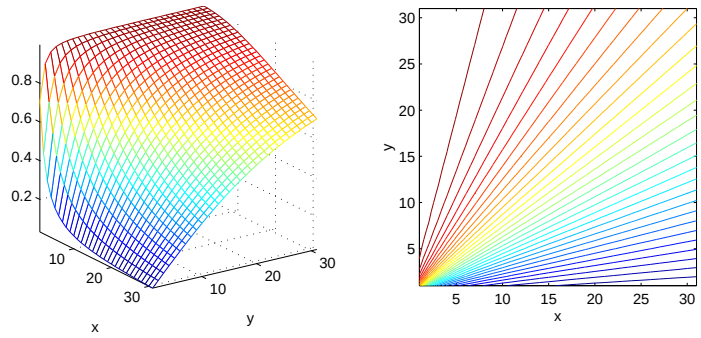

Figure 1: $f = \cos\alpha$.

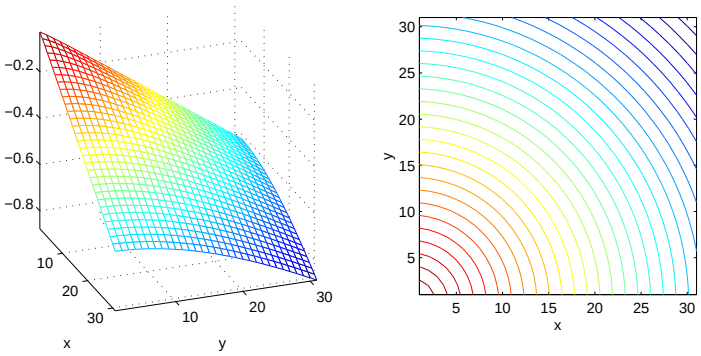

Figure 2: $f = -\sqrt{x^2 + y^2}$.

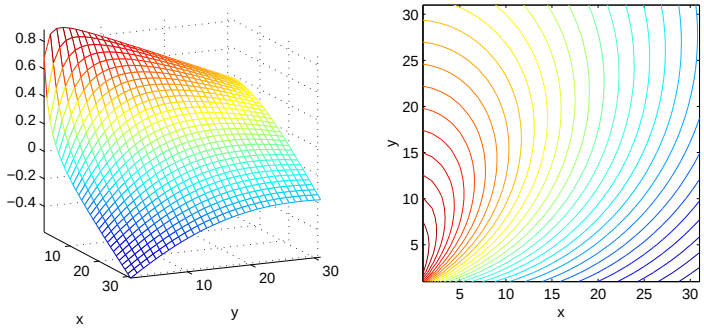

Figure 3: $f = \cos\alpha - \sqrt{x^2 + y^2}$.

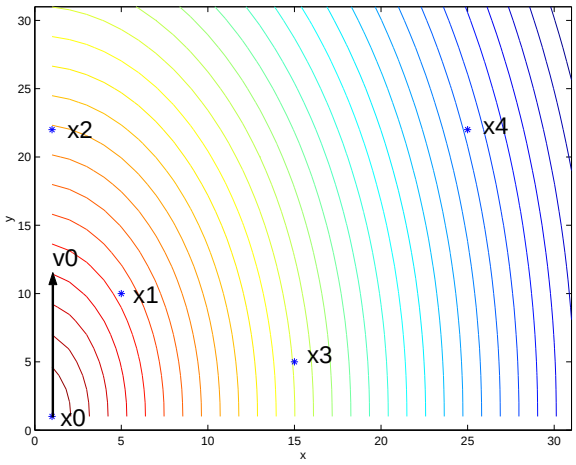

Figure 4: Example of stencil choice, $f = -\sqrt{x^2 + (y/2)^2}$.

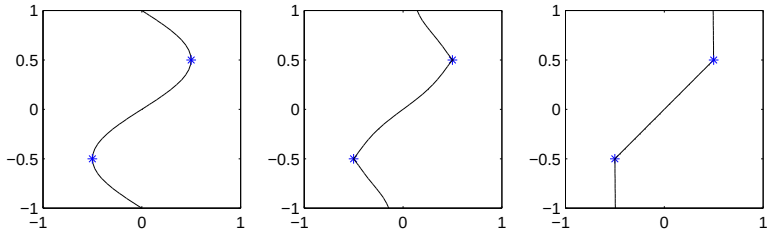

Figure 5: Minimal surface evolution in 2d with 2 point boundary Γ denoted by the * points. At $t = 0, 0.16, 0.8$.

3.3 Reinitialization

As is done on the points of $\bar{\Omega}$ away from Γ, we evolve (5) for a few iterations after each timestep that (3) is advanced. We use the same technique as is done in section 3.2 to construct the stencil S_0, but then instead of using central differencing to approximate derivatives of Φ we use one sided upwind finite differencing where it is needed in the Godunov solver of (5). This means that when the numerical Hamiltonian that is used to approximate $|\nabla\varphi|$ calls for $D^+_{x_i}\varphi,\ D^-_{x_i}\varphi$ we will use $(\Phi(x_0 + e_i h) - \Phi(x_0))/h,\ (\Phi(x_0) - \Phi(x_0 - e_i h))/h$, respectively.

4 Numerical Examples

In this section we show numerical results.

In 2d with Γ being a set of 2 points the minimal surface will be a line, as in figure 5. We use a uniform cell width of $dx = 0.04$.

In 3d an example where we can compare our solution with an analytic result is when Γ is given by two circles defined by $x^2 + y^2 = 0.5^2,\ z = \pm 0.277259$. This example was also computed in [3]. The initial condition is a cylinder $x^2 + y^2 = 0.5^2$. In this example we use the symmetry of the solution to reduce the computational domain to the space $x, y \in [0, 0.7],\ z \in [0, 0.35]$, where we use a uniform cell width of $dx = 0.035$. The minimal surface boundary Γ is thus a quarter circle which is discretized using 1000 equispaced points that lie in the computational domain. However, after the stencils are chosen only 191 of these points are used.

The exact solution is a catenoid with radius $r(z) = 0.4\cosh(z/0.4)$, whose radius at $z = 0$ is 0.4. We can measure the radius at $y = 0, z = 0$ to be $r = 0.3936$ which gives an error of 0.0064 which is on the order of dx^2.

Note that because of the symmetric nature of the Neumann BCs imposed we are also computing the solution of a catenoid where Γ is given by 2 circles defined by $x^2 + y^2 = 0.5^2,\ z = 0.35 \pm (0.35 - 0.277259)$.

Another 3d example is found by letting Γ lie on Enneper's minimal surface.

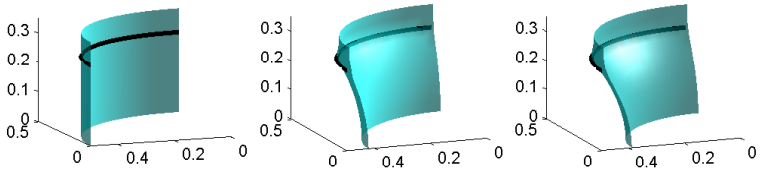

Figure 6: Minimal surface evolution in 3d with 2 circle boundary Γ denoted by the dark line. At $t = 0, 0.123, 0.367$.

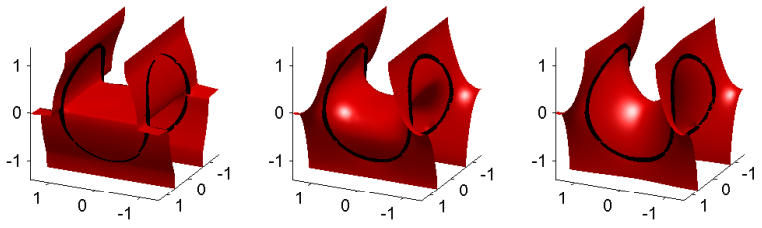

Figure 7: Minimal surface evolution in 3d with Enneper surface boundary Γ denoted by the dark line. At $t = 0, 0.063, 0.439$.

For this example we use the parameterization of Enneper's surface

$$\{x, y, z\} = \{r\cos\theta - \frac{1}{3}r^3\cos(3\theta), -r\sin\theta - \frac{1}{3}r^3\sin(3\theta), r^2\cos(2\theta)\}$$

is used. For Γ we take $r = 1,\ \theta \in [-\pi, \pi)$ for 2000 equispaced points in θ. The resulting curve resembles the stitching pattern on a baseball. After the stencils are chosen 1618 of these points are used. The computational domain is $[-1.4, 1.4]^3$ and the uniform space step size is $2.8/50$. The initial surface has the same topology as Enneper's surface, and consists of piecewise planar and cylindrical surfaces that have Gaussian curvature $= 0$ almost everywhere.

We show 2 different views of the evolution in figures 7, 8, and a comparison with the exact solution in figure 9. Only the surface inside Γ should be compared with the exact solution.

In 4d we compute a generalized catenoid solution where Γ is defined as 2 spheres given by $x^2+y^2+z^2 = 0.5^2,\ w = \pm 0.2$. The initial condition is a hyper-cylinder $x^2+y^2+z^2 = 0.5^2$. In this example we use the symmetry of the solution to reduce the computational domain to the space $x, y, z \in [0, 0.6],\ w \in [0, 0.3]$, where we use a uniform cell width of $dx = 1/30$. The minimal surface boundary Γ is thus an eighth of a sphere that is discretized using $41,692$ approximately equispaced points that lie in the computational domain. However, after the stencils are chosen only 8051 of these points are used.

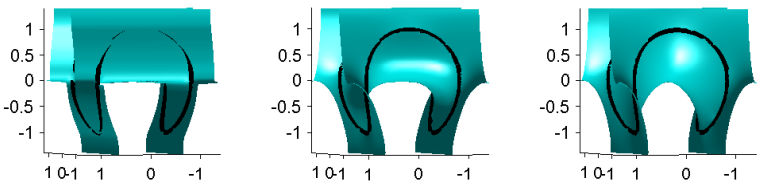

Figure 8: Minimal surface evolution in 3d with Enneper surface boundary Γ denoted by the dark line. At $t = 0, 0.063, 0.439$.

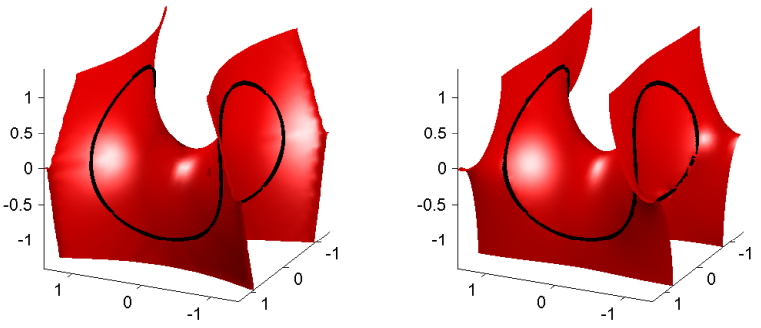

Figure 9: Minimal surface evolution in 3d with Enneper surface boundary Γ denoted by the dark line. Left: exact solution. Right: computed solution at $t = 0.439$.

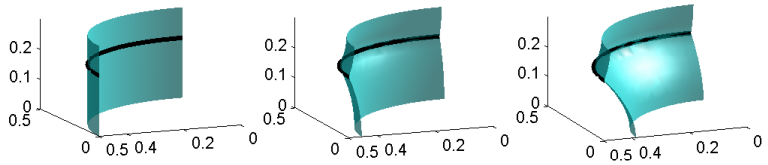

Figure 10: Minimal surface evolution in 4d with 2 sphere boundary Γ denoted by the dark line. Slices taken at $x = 0$, at $t = 0, 0.034, 0.411$.

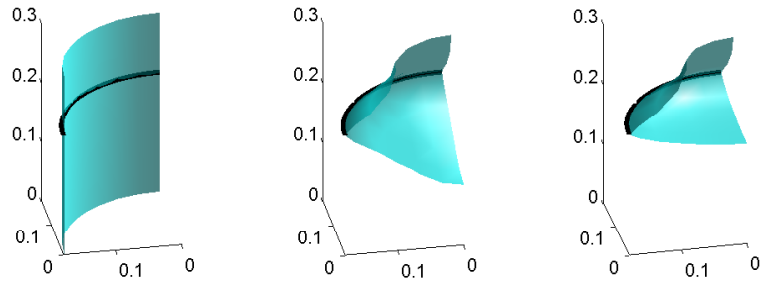

Figure 11: Minimal surface evolution in 4d with 2 sphere boundary Γ denoted by the dark line. Slices taken at $x = 0.4\bar{6}$, at $t = 0, 0.034, 0.411$.

Note that because of the symmetric nature of the Neumann BCs imposed we are also computing the solution of a catenoid where Γ is given by 2 spheres defined by $x^2 + y^2 + z^2 = 0.5^2,\ w = 0.3 \pm 0.1$.

We show 3d slices of the solution for fixed values of x at various times. Slices taken for fixed y, z values look identical to those shown, and the slices for fixed w values look like spheres.

Note how in the slice taken when $x = 0.4\bar{6}$ that the surface remains a catenoid when $|w| > 0.2$, but has changed topology in the region $|w| < 0.2$.

5 Conclusion

In this paper we introduce a numerical method for computing minimal surfaces in arbitrary dimension that have codimension-2 boundary, Γ, by evolving an initial codimension-1 surface by mean curvature flow. The method uses existing finite differences techniques away from Γ, and a new evolution procedure using radial basis functions near Γ. The method used is dimension independent and computed examples are shown in $2, 3$ and 4 dimensions.

Future work can include the study of unstable minimal surfaces. Surfaces with generalized triple points can also be studied, perhaps by the use of multiple level set functions [17]. As computer memory and speed increase higher

dimensional problems will also be approached. The method presented can also be applied to other non-linear evolutions with irregular fixed boundaries in arbitrary codimension.

Acknowledgments This work is supported by NSF grants DMS-0312222 and ACI-0321917, and an ONR MURI grant, subcontracted from Stanford University.

References

[1] Kenneth A. Brakke. The surface evolver. *Experiment. Math.*, 1(2):141–165, 1992.

[2] T. Cecil, J.L. Qian, and S. Osher. Numerical methods for high dimensional Hamilton-Jacobi equations using radial basis functions. *J. Comput. Phys.*, 196:327–347, 2004.

[3] David L. Chopp. Computing minimal surfaces via level set curvature flow. *J. Comput. Phys.*, 106(1):77–91, 1993.

[4] C. Coppin and D. Greenspan. A contribution to the particle modeling of soap films. *Appl. Math. Comput.*, 26(4):315–331, 1988.

[5] Ulrich Dierkes, Stefan Hildebrandt, Albrecht Küster, and Ortwin Wohlrab. *Minimal surfaces. I,II*, volume 295,296 of *Grundlehren der Mathematischen Wissenschaften [Fundamental Principles of Mathematical Sciences]*. Springer-Verlag, Berlin, 1992. Boundary regularity.

[6] Jesse Douglas. A method of numerical solution of the problem of Plateau. *Ann. of Math. (2)*, 29(1-4):180–188, 1927/28.

[7] G. Dziuk. An algorithm for evolutionary surfaces. *Numer. Math.*, 58(6):603–611, 1991.

[8] Gerhard Dziuk and John E. Hutchinson. On the approximation of unstable parametric minimal surfaces. *Calc. Var. Partial Differential Equations*, 4(1):27–58, 1996.

[9] Gerhard Dziuk and John E. Hutchinson. The discrete Plateau problem: algorithm and numerics. *Math. Comp.*, 68(225):1–23, 1999.

[10] Donald Greenspan. On approximating extremals of functionals. I. The method and examples for boundary value problems. *ICC Bull.*, 4:99–120, 1965.

[11] Michael Hinze. On the numerical approximation of unstable minimal surfaces with polygonal boundaries. *Numer. Math.*, 73(1):95–118, 1996.

[12] Ronald H. W. Hoppe. Multigrid algorithms for variational inequalities. *SIAM J. Numer. Anal.*, 24(5):1046–1065, 1987.

[13] Johannes C. C. Nitsche. *Lectures on minimal surfaces. Vol. 1.* Cambridge University Press, Cambridge, 1989. Introduction, fundamentals, geometry and basic boundary value problems, Translated from the German by Jerry M. Feinberg, With a German foreword.

[14] S.J. Osher and J.A. Sethian. Fronts propagating with curvature dependent speed: algorithms based on Hamilton-Jacobi formulations. *Journal of Computational Physics*, 79:12–49, 1988.

[15] Stanley Osher and Ronald P. Fedkiw. *Level Set Methods and Dynamic Implicit Surfaces.* Oxford Univ. Press, 2002.

[16] Harold R. Parks. Explicit determination of area minimizing hypersurfaces. II. *Mem. Amer. Math. Soc.*, 60(342):iv+90, 1986.

[17] Luminita Vese and Tony Chan. A multiphase level set framework for image segmentation using the mumford and shah model. *Int. J. of Computer Vision*, 50(3):271–293, 2002.

[18] H.-J. Wagner. A contribution to the numerical approximation of minimal surfaces. *Computing*, 19(1):35–58, 1977/78.